Comparison of 18F-fluoro-deoxy-glucose, 18F-fluoro-methyl-choline, and 18F-DPA714 for positron-emission tomography imaging of leukocyte accumulation in the aortic wall of experimental abdominal aneurysms

Laure Sarda-Mantel, MD, PhD,[a,b,c] Jean-Marc Alsac, MD,[a] Raphaël Boisgard, PhD,[d,e] Florence Hervatin, PhD,[b] Françoise Montravers, MD, PhD,[f] Bertrand Tavitian, MD, PhD,[d,e] Jean-Baptiste Michel, MD, PhD,[a] and **Dominique Le Guludec, MD, PhD,[a,b,c]** *Paris and Orsay, France*

Objective: **Abdominal aortic aneurysm (AAA) is a frequent form of atherothrombotic disease, whose natural history is to enlarge and rupture. Indicators other than AAA diameter would be useful for preventive surgery decision-making, including positron-emission tomography (PET) methods permitting visualization of aortic wall leukocyte activation relevant to prognostic AAA evaluation. In this study, we compare three PET tracers of activated leukocytes, 18F-fluoro-deoxy-glucose (FDG), 18F-fluoro-methyl-choline (FCH), and 18F-DPA714 (a peripheral benzodiazepine receptor antagonist) for in vivo PET quantification of aortic wall inflammation in rat experimental AAAs, in correlation with histopathological studies of lesions.**

Methods: **AAAs were induced by orthotopic implantation of decellularized guinea pig abdominal aorta in 46 Lewis rats. FDG-PET (n = 20), FCH-PET (n = 8), or both (n = 12) were performed 2 weeks to 4 months after the graft, 1 hour after tracer injection (30 MBq). Six rats (one of which had FDG-PET) underwent 18F-DPA714-PET. Rats were sacrificed after imaging; AAAs and normal thoracic aortas were cut into axial sections for quantitative autoradiography and histologic studies, including ED1 (macrophages) and CD8 T lymphocyte immunostaining. Ex vivo staining of AAAs and thoracic aortas with 18F-DPA714 and unlabeled competitors was performed.**

Results: **AAAs developed in 35 out of 46 cases. FCH uptake in AAAs was lower than that of FDG in all cases on imaging, with lower AAA-to-background maximal standardized uptake value (SUV_{max}) ratios (1.78 ± 0.40 vs 2.71 ± 0.54; $P < .01$ for SUV_{max} ratios), and lower AAA-to-normal aorta activity ratios on autoradiography (3.52 ± 1.26 vs 8.55 ± 4.23; $P < .005$). FDG AAA-to-background SUV_{max} ratios correlated with the intensity of CD8 + ED1 staining ($r = .76$; $P < .03$). FCH AAA-to-background SUV_{max} ratios correlated with the intensity of ED1 staining ($r = .80$; $P < .03$). 18F-DPA714 uptake was similar in AAAs and in normal aortas, both in vivo and ex vivo.**

Conclusions: **In rat experimental AAA, characterized by an important aortic wall leukocytes activity, FDG-PET showed higher sensitivity than FCH-PET and 18F-DPA714-PET to detect activated leukocytes. This enhances potential interest of this tracer for prognostic evaluation of AAA in patients. (J Vasc Surg 2012;56:765-73.)**

Clinical Relevance: **The decision for preventive surgery of abdominal aortic aneurysm (AAA) is based on clinical signs and AAA diameter. However, AAA progression is not linear; growth acceleration usually precedes rupture. Therefore, other indicators of lesion development would be useful for surgical decision-making. Adventitial inflammation has been linked to AAA enlargement. Therefore, positron-emission tomography (PET) imaging quantifying activated leukocytes in aortic wall could be useful for prognostic evaluation of AAAs. In this experimental study comparing three main PET tracers of activated leukocytes, we show that 18F-fluoro-deoxy-glucose has the highest sensitivity of detection and appears the most promising for clinical use in this setting.**

From the Institut National de la Santé et de la Recherche Médicale Unit 698,[a] the Université Paris Diderot,[b] and the Service de Médecine Nucléaire, Hôpital Bichat, APHP,[c] Paris; the Service Hospitalier Frédéric Joliot, Commissariat à l'Energie Atomique,[d] and the Institut National de la Santé et de la Recherche Médicale Unit 1023, Université Paris Sud,[e] Orsay; and the Laboratoire d'Imagerie Moléculaire Positonique (LIMP), Hôpital Tenon et Université Pierre and Marie Curie, Paris.[f]

Institut National de la Sante et de la Recherche Medicale Unit 698 is supported by the European Union integrated FP-7 program FAD (HEALTH-F2-2008-200647, http://www.fighting-aneurysm.org/), and by a grant of the Fédération Française de Cardiologie.

Author conflict of interest: none.

Reprint requests: Dr Laure Sarda-Mantel, Service de Médecine Nucléaire, Hôpital Bichat, 46 rue Henri Huchard, 75018 Paris, France (e-mail: laure.sarda@inserm.fr).

The editors and reviewers of this article have no relevant financial relationships to disclose per the JVS policy that requires reviewers to decline review of any manuscript for which they may have a conflict of interest.

0741-5214/$36.00

doi:10.1016/j.jvs.2012.01.069

Abdominal aortic aneurysm (AAA) is a frequent form of atherothrombotic disease, anatomically characterized by focal dilatation resulting in an expanded, beating abdominal mass.[1,2] Currently, the decision for preventive surgery is based on clinical signs and anatomic criteria: a diameter superior to 5.5 cm, or a diameter increase on echography or computed tomography (CT). However, AAA progression is not linear,[3,4] and growth acceleration usually precedes rupture. Therefore, indicators of lesion development other than AAA diameter would be useful for surgical decision-making.

Many biological processes, including activity of parietal thrombus,[5] adventitial innate, and adaptive immune response[6] angiogenesis and activity of proteases, have been linked to AAA enlargement. That is why, besides anatomic imaging, molecular imaging targeting these biological processes could have a potential interest for patients' management. Positron-emission tomography (PET) imaging permitting quantification of leukocytes extravasations and accumulation in aortic wall could be especially useful for prognostic evaluation of AAAs.[7]

Currently, three PET tracers of inflammatory cells are candidates for clinical use in atherosclerosis: 18F-fluorodeoxy-glucose (FDG), 18F-fluoro-methyl-choline (FCH), and 18F-DPA714 (DPA), a peripheral benzodiazepine receptor antagonist. FDG is a radiotracer of cellular glucose metabolism, with high sensitivity of detection in malignant tumors and inflammatory diseases (96% in mild chronic septic inflammation).[8] Despite controversial specificity with regard to arterial wall leukocyte content,[9] which has been related to occurrence of clinical events, it is actually under intense clinical investigation in atheroma and AAAs as a prognostic marker.[10-13] FCH, which targets choline transport and cell membrane incorporation, is clinically used to detect prostate cancers. It can detect inflammatory cells in murine and human atherosclerosis,[14,15] but its sensitivity has not been evaluated in patients. High-affinity radioligands specific for peripheral benzodiazepine receptors, including 18F-DPA714, have been successfully used to target tissue leukocytes in animal models of neuroinflammation.[16,17] Their sensitivity for the detection of inflammatory diseases in patients has not been evaluated.

The aim of the present work was to compare the sensitivity of these three tracers for the detection of aortic wall leukocytes accumulation in vivo in an experimental model of immune-induced aortic aneurysm in rats,[18] and to verify their specificity with regard to leukocytes content. The results of this preclinical study will guide further clinical study in this setting.

METHODS

Animal model

Experimental AAAs were induced by the orthotopic implantation of a segment (1.5 cm) of sodium dodecyl sulfate (SDS)-decellularized guinea pig abdominal aorta (xenogenic matrix) in Lewis rats, under anesthesia (50 mg/kg intraperitoneal injection [IP] ketamine [Imalgène 500; Merial, Lyon, France] and 10 mg/kg IP xylazine [2% Rompun, Bayer, Puteaux, France]), according to the previously described method.[18] The procedure and the animal care complied with the principles formulated by the National Society for Medical Research. This study was performed under the authorization # 75-214 of the French Ministry of Agriculture. The host's immunoinflammatory responses to the engrafted extracellular matrix induce vascular remodeling leading to formation of an aneurysm with an intraluminal thrombus.[19] This xenograft model is characterized by important accumulation of $CD8^+$ lymphocytes and macrophages within the grafted aortic wall,[20,21] which is at maximum at 2 weeks then decreases while AAA diameter increases. Also, the activation markers ICAM-1 and LFA-1 correlate with the density of total inflammatory cells,[20] and are at maximum at day 15 then decrease. Therefore, it is relevant to the adventitial immune response observed in outer media and adventitia of human AAA.[6]

PET imaging

PET imaging was performed at different times after the graft, from early phase (11-14 days) to several months, to be able to verify a correlation between the intensity of PET signal and the density of inflammatory cells in the aneurysmal parietal wall (specificity of the targeting). FDG-PET and FCH-PET were performed on the same imaging device in Tenon Laboratory. Dual FDG- and FCH-PET was planned in 20 animals for direct comparison of performances, but it could only be performed in 12 rats because of frequent timely delivery issues for FCH (only FDG-PET was done). Additional rats were used with either FDG or FCH for the correlation between PET imaging and immunohistology. For legal reasons, DPA-PET imaging was performed on the site of tracer production (Orsay).

18F-FDG

FDG-PET was performed once in 32 operated rats, from 11 days to 4 months after the graft. Four sham-operated rats also underwent FDG imaging. PET examinations were performed on a Mosaic small animal PET (Philips, Cleveland, Ohio). This system has a 2.2-mm resolution at the center of the field of view. The energy window was 450 to 700 keV, and the coincidence timing window was 6 ns. Data were acquired in 3D mode and corrected for decay and randoms. A single bed acquisition was sufficient to image the whole abdomen and pelvis of animals. Reconstruction was performed using the 3D row action maximum likelihood algorithm. Attenuation correction was not applied. Following at least 6 hours fasting, the rats under anesthesia (2% isoflurane in 100% O2) received an average activity of 30 MBq of FDG (Flucis [Cis Bio, Orsay, France] or Efdege [Iason, Seiersberg, Austria]) through a vein injection. The residual dose was measured to verify the effective dose injected. Before, during, and after FDG injection, animals were kept under an infrared light to minimize brown fat visualization. PET examinations (static acquisition of 20-minute duration) were performed 1 hour after injection.

18F-FCH

FCH-PET was performed in 20 operated rats, from 2 weeks to 4 months after the graft, including 12 that also had FDG-PET the day before (six rats) or after (six rats) FCH-PET, on the same microPET device, using the same protocol except that three static images of 20-minutes duration were performed at 20 minutes, 40 minutes, and 1 hour after FCH injection (30MBq Iasocholine [Iason]), to determine the time of highest signal-to-noise ratio.

18F-DPA714

DPA-714N,N-diethyl-2-(2-(4-(2-fluoroethoxy)phenyl)-5,7-dimethylpyrazolo[1,5-a]pyrimidine-3-yl)acetamide was labeled with fluorine-18 using a tosyloxy-for-fluorine nucleophilic aliphatic substitution. This simple one-step process involves reaction of K-^{18}F-F-Kryptofix222 with the tosyloxy precursor (4.5-5.0 mg, 8.2-9.1 μmol) at 165°C for 5 minutes in dimethyl sulfoxide (0.6 mL), followed by C-18 PrepSep cartridge (Fisher Scientific, Strasbourg, France) prepurification, and finally semipreparative high-pressure liquid chromatography purification on an X-Terra RP18 (Waters, Guyancourt, France). 18F-DPA714 (>95% radiochemically pure) was obtained within 90 minutes of radiosynthesis with specific radioactivity of 185 MBq/μmol. Six grafted rats (one of which had FDG-PET the day before) underwent 18F-DPA714-PET on an ECAT high-resolution research tomograph PET system (Siemens Medical Solutions, Knoxville, Tenn, spatial resolution 2.3 mm), 2 weeks to 1 month after the graft. 18F-DPA714 (20 MBq) was injected into anesthetized rats (2% isoflurane in 100% O2), and mod-list whole-body PET acquisition was performed from the time of injection to 3 hours and 30 minutes postinjection. Then, 10 images of 20-minute duration were reconstructed from mod-list acquisition, including one at 1 hour postinjection. The raw data were reconstructed using an ordered subset expectation maximization weighted attenuation with six iterations and eight sub subsets, including a Fourier rebinning.

Data analysis. PET images were considered positive (visual analysis) when increased tracer uptake was seen in the abdominal aortic aneurysmal wall compared with the subjacent normal aorta. Quantification was performed on the 20-minute duration images obtained 1 hour after injection of the tracers. Two-dimensional regions of interest (ROIs) were drawn on the infrarenal aortic wall (when visible) and in surrounding soft tissue (background activity). Maximal standard uptake values (SUV_{max}; ratio of tissue radioactivity concentration [kBq/mL] at time t and injected dose [MBq] at the time of injection divided by body weight [kg]) were determined in ROIs, and SUV_{max} ratio between the aortic wall and surrounding soft tissue was calculated for each axial slice. For data analysis, we used the mean value obtained for SUV_{max} and AAA/background SUV_{max} ratio in four consecutive axial slices. The latter parameter is derived from that validated for quantification of inflammation with FDG-PET in carotid atherosclerotic plaques of patients.[11,22]

Autoradiography

All rats were sacrificed after imaging. A ring of the thoracic and the infrarenal aortas were dissected out, frozen, and cut into transverse sections of 20-μm thickness, which were exposed in a radioimager (Instant Imager, Packard Instrument Co, Meriden, Conn) for 16 hours. The activity (total counts per section) was determined on autoradiograms.

Also, axial and transversal sections of AAA and normal thoracic aorta of three noninjected rats were incubated with either 18F-DPA714, 18F-DPA714 mixed with a 100-fold excess of PK11195 (another peripheral benzodiazepine receptor [PBR] antagonist), or 18F-DPA714 mixed with an excess (20 mmol) of unlabeled DPA714, for ex-vivo radiolabeling of leukocytes. Sections were incubated for 20 minutes in Tris Buffer (Sigma, Saint-Quentin Favallier, France), adjusted at pH 7.4 at 41°C, and then rinsed for 2 minutes with cold buffer, followed by a quick wash in cold distilled water. Sections were then placed in direct contact with a Storm 860 Phosphor-Imager screen (GMI Inc, Ramsey, Minn) and exposed overnight. Autoradiograms were analyzed using the ImageQuant software (GMI Inc).

Histologic studies

Sections used for autoradiography were stained with hematoxylin-eosin. Immunostaining for rat CD8 T lymphocytes (anti-CD8, AbD Serotec, Düsseldorf, Germany) and rat macrophages (anti-ED1, AbD Serotec) was performed on 8-μm tissue sections, according to the manufacturer's instructions. Immunostaining of all rat sections was performed at the same time. Briefly, tissue sections were fixed in acetone, treated by TRIS EDTA at 95°C for 30 minutes, then H_2O_2 for 1 hour, avidin biotin for 10 minutes, and finally 1% bovine serum albumin in TRIS for 40 minutes. The primary Ab anti-ED1 (1/100) or anti-CD8 (1/50) was applied overnight. After rinsing, the secondary Ab (BA2001 1/1000 et al 1/100) was applied and then revealed with 3,3'-diaminobenzidine (10 minutes). Positive controls using rat spleen sections and negative controls using mouse IgG1 instead of anti-ED1 and anti-CD8 primary antibodies were performed simultaneously. The number of positive cells per mm^2 of myocardial section was estimated by light microscope at 400-fold magnification in one section per rat, using Histolab quantification software.

Statistical analysis

Comparison of SUV_{max} and signal-to-noise ratios on PET images, as well as of AAA-to-normal aorta activity ratios on autoradiography, were performed between animals with AAAs and sham-operated rats, and between FDG and FCH, using the Student *t*-test. The level of significance was set at 0.05. A correlation regression test was used to compare the distributions of SUV_{max} or AAA-to-background SUV_{max} ratios and those of AAA diameter, time after the graft, and ED1 or CD8 quantifications.

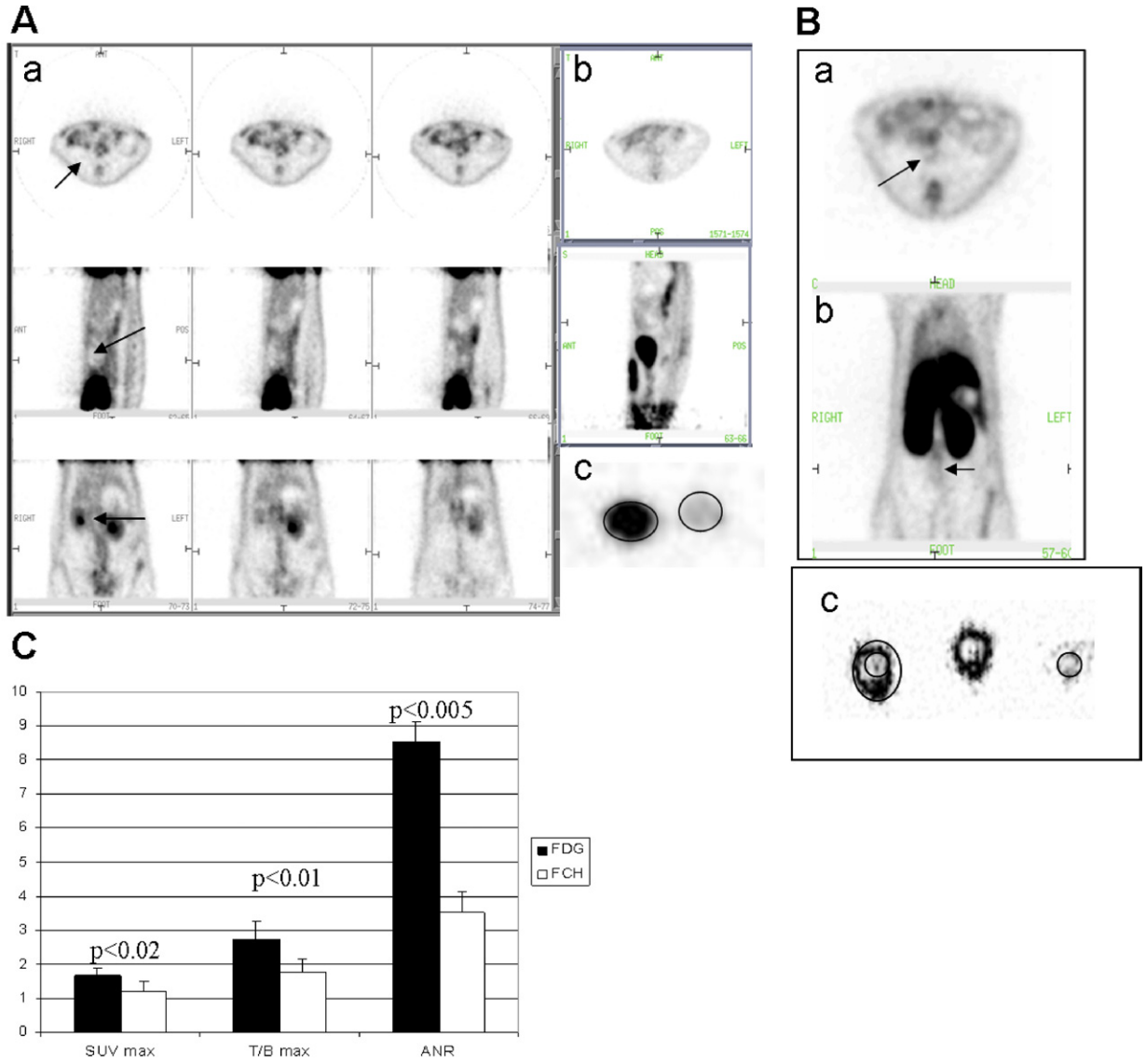

Fig 1. A, Positive fluoro-deoxy-glucose (*FDG*)-positron-emission tomography (PET) in a rat with abdominal aortic aneurysm (AAA). **a,** FDG-PET imaging in a rat with AAA. Increased FDG uptake (*arrows*) is seen in AAA parietal wall compared with normal aorta. **b,** FDG-PET in a sham-operated rat; no increased FDG uptake is observed in normal abdominal aorta. **c,** Autoradiography of AAA (*left*) and normal aorta (*right*); intense FDG uptake is observed in AAA. **B,** Positive fluoro-methyl-choline (*FCH*)-PET in a rat with AAA (*arrow*). **a,** PET axial view. **b,** PET frontal view. **c,** Autoradiography of AAA (*left*) and normal aorta (*right*). Activity ratio between AAA and normal aorta sections is 3.1. **C,** Comparison of FDG and FCH uptakes on PET imaging* and autoradiography. FCH uptake in AAA parietal wall is lower than that of FDG, with lower SUV_{max} and T/B ratios on PET imaging, as well as lower ANR on autoradiography. *ANR*, AAA-to-normal thoracic aorta activity ratio on autoradiography; *T/B*, AAA-to-background SUV_{max} ratio on PET imaging. *FDG and FCH imaging in the same rats.

RESULTS

AAAs developed in 35 of 46 operated rats (diameter, 2-15 mm; length, 7-20 mm; control diameter, 1.1 mm). The transaxial diameter of AAAs imaged with both FDG and FCH was similar to that of AAAs imaged with DPA (4.4 ± 1.5 vs 4.3 ± 0.4 mm; P = NS).

Twenty-eight of the 32 rats that underwent FDG-PET had an AAA at sacrifice. Visual analysis of images revealed increased FDG uptake in AAA wall in 25 cases (SUV_{max} 1 hour postinjection, 1.73 ± 0.53; Fig 1, *Aa*), and no increase in three cases (SUV_{max}, 1.04 ± 0.18; AAAs of 4-5 mm diameter). SUV_{max} was 0.9 ± 0.1 in infrarenal aorta of grafted rats with no AAA. SUV_{max} in background tissue surrounding abdominal aorta was 0.60 ± 0.12.

Fifteen of the 20 rats that underwent FCH imaging had an AAA at sacrifice. Visual analysis of images revealed

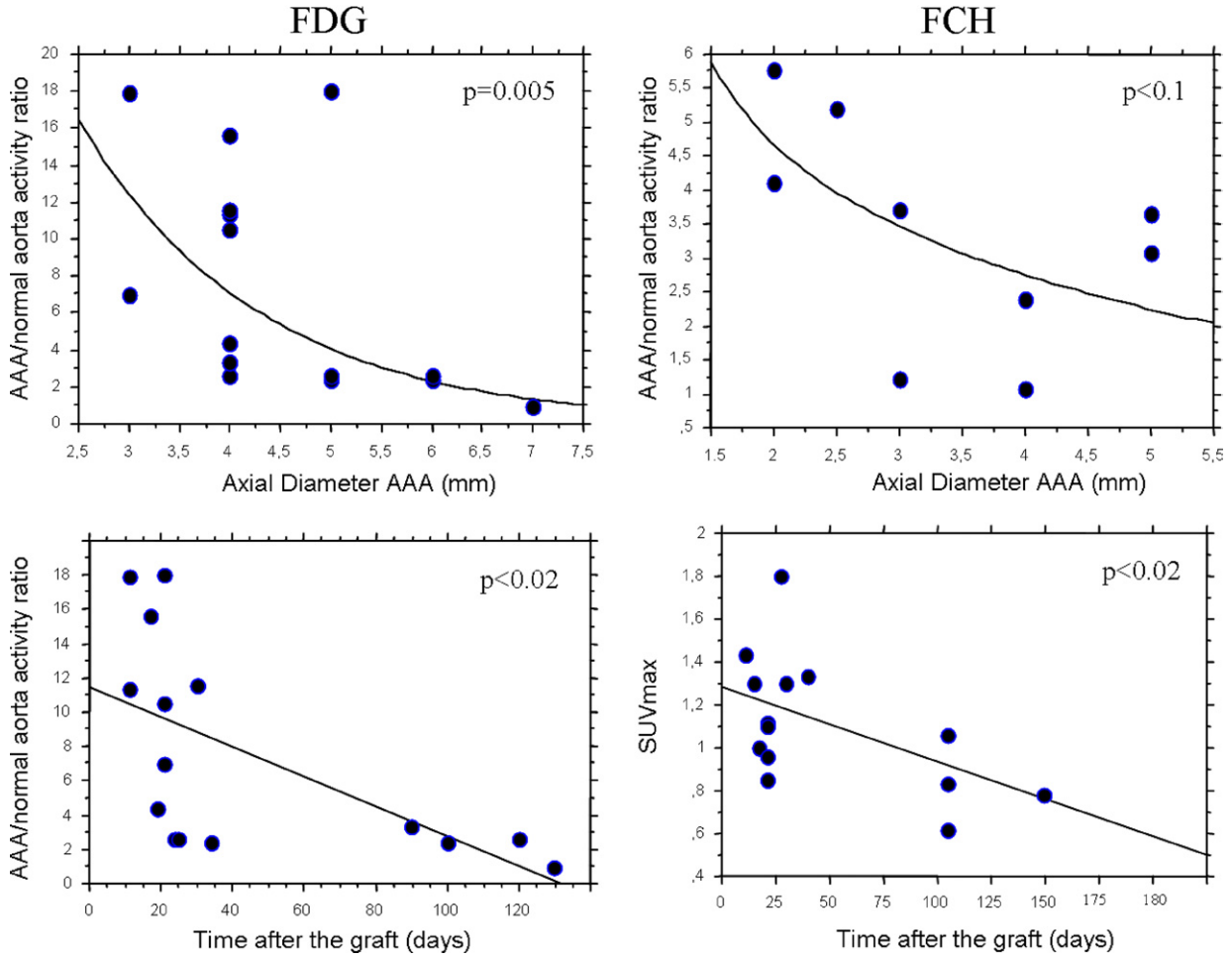

Fig 2. Evolution of fluoro-deoxy-glucose (*FDG*) (*left column*) and fluoro-methyl-choline (*FCH*) (*right column*) uptakes in abdominal aortic aneurysms (*AAAs*) as function of AAA diameter and time after the graft.

increased FCH uptake in AAA wall in 10 of 15 AAAs, which was not modified between 20 minutes and 1 hour postinjection (SUV_{max} 1 hour postinjection, 1.31 ± 0.33; Fig 1, *Bb*), and no increase in five rats (SUV_{max} 1 hour postinjection, 0.83 ± 0.16; 3-8 mm diameter). SUV_{max} was 0.5 ± 0.1 in infrarenal aorta of grafted rats with no AAA. SUV_{max} in background tissue surrounding abdominal aorta was 0.64 ± 0.05. In the 12 rats that underwent both FCH and FDG imaging, FCH uptake in AAA was lower than that of FDG on visual analysis of PET images (Fig 1, *Ba* and *Bb*), including two AAAs with negative FCH scan and positive FDG scan; and both SUV_{max} in AAAs and AAA-to-background SUV_{max} ratios on FCH-PET were lower than on FDG-PET (Fig 1, *C*).

Autoradiographic studies demonstrated that FDG and FCH activity were located in the AAA wall (Fig 1, *Ac* and *Bc*). FCH AAA-to-normal aorta activity ratios on autoradiography were lower than that of FDG (Fig 1, *C*).

Globally, uptake of both FDG and FCH in parietal walls of AAAs (measured on PET images or autoradiography) decreased with AAA diameter and with time after the graft (Fig 2).

All six rats injected with 18F-DPA714 had AAA, and all had negative PET images. One of them also underwent FDG-PET, which was positive. 18F-DPA714 uptake in AAAs was not different from that observed in the wall of control normal aortas (Fig 3, *A*). This was confirmed by autoradiography, which demonstrated significant tracer activity in the wall of both AAA and normal thoracic aorta, with 18F-DPA714 aneurysm-to-normal aorta activity of only 2.0 ± 0.4. Ex vivo studies confirmed tracer binding to both AAA and normal aortic wall, which was inhibited by 11C-PK11195, and unlabeled DPA714 (Fig 3, *B*).

Immunohistological studies demonstrated ED1+ monocyte-macrophages and $CD8^+$ T lymphocytes in the adventitia of all AAAs (Fig 4). ED1 staining varied from 190 to 2194 positive cells per AAA sections, CD8 staining varied from 6 to 2029, and total stained cells per section varied from 428 to 6342. We found a significant correlation between FDG SUV_{max} or AAA-to-background SUV_{max} ratios and the number total stained cells (CD8 + ED1) reflecting numbers of both macrophages and $CD8^+$ T lymphocytes in the AAA section ($r = .76$; $P < .03$;

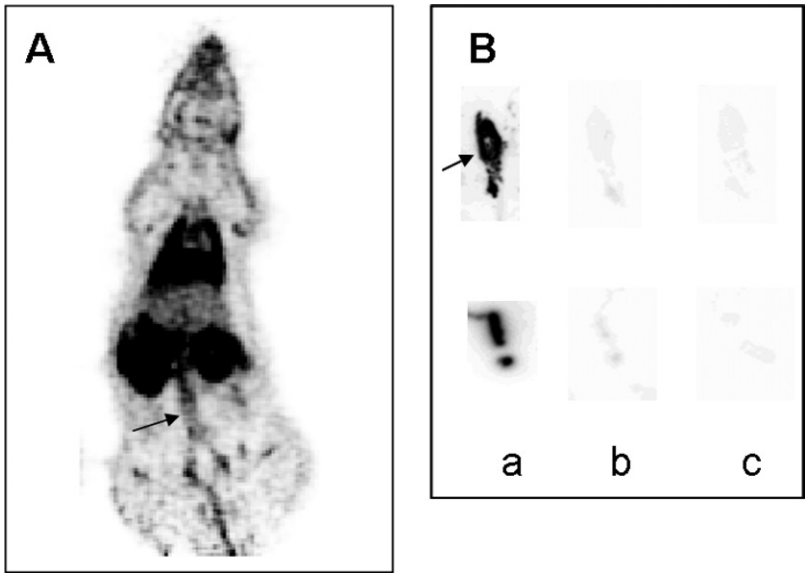

Fig 3. Examples of 18F-DPA714 positron-emission tomography (PET) and autoradiographic data. **A,** 18F-DPA714 PET frontal view of a rat with inflamed abdominal aortic aneurysm (AAA), 30 to 60 minutes postinjection; similar tracer uptake is observed in AAA and subjacent iliac arteries. **B,** Ex vivo labeling of AAA (*upper panel*) and normal aorta (*lower panel*) in another rat; high 18F-DPA714 uptake is observed in both tissues with comparable intensity **(a)**, which disappears in the presence of unlabeled PK11195 **(b)** or DPA714 **(c)**, indicating specific labeling of peripheral benzodiazepine receptors in both AAA and normal aorta wall.

Fig 4). No significant correlation was found between FDG-SUV_{max} and ED1, or CD8 staining separately. Using FCH, AAA-to-background SUV_{max} ratio significantly correlated with ED1 (macrophages) staining ($r = .80$; $P < .03$; Fig 5). AAAs with negative FDG-PET that were quantified (n = 2) had 428 and 531 stained cells per section; one with negative FCH-PET had 926 stained cells per section. Grafted rats with no AAA that were quantified had 467 and 3342 stained cells per section of infrarenal aorta.

DISCUSSION

In this rat model of AAA (aortic xenograft), FDG- and FCH-PET signals in the AAA wall correlated significantly with the quantity of macrophages and CD8 lymphocytes. FDG uptake in AAAs was higher than that in normal aorta in all cases, and higher than that of FCH uptake. 18F-DPA714-PET was not significantly different in AAAs and in normal aorta.

18F-FDG imaging of inflammatory lesions. Glucose and FDG uptake are increased in activated monocytes and lymphocytes.[23,24] FDG accumulation correlates with the number and activity of gluclose transporters (GLUT) 1 and GLUT 3.[24] Expression of GLUT 1 and GLUT 3 is augmented 3.5- and six-fold, respectively, in lymphocytes following activation by phytohemagglutinin.[23] GLUT 1 expression is increased two-fold in monocytes upon activation with lipopolysaccharide, with a two- to three-fold increase in glucose influx.[23] In vivo, it has been shown in mouse models of chronic enterocolitis that the FDG signal is only related to activated T lymphocytes and not to nonactivated ones.[25] As observed in our experimental AAAs, significant FDG uptake was reported in human AAAs, corresponding to adventitial lymphocyte granuloma on histology, whereas the mural thrombus was FDG-negative.[12,13] Many authors have studied the relation between FDG uptake in leukocyte-rich lesions and the presence of either monocyte-macrophages, CD4 lymphocytes, or CD8 lymphocytes in atherothrombotic plaques,[26-28] mammary tumors, and chemotherapy-induced pneumopathies, with various and sometimes discordant results. In a recent experimental study, discrepancies were found between signals measured on atherosclerotic aortic wall with N1177, a CT marker of phagocytic cells, and FDG-PET.[27] Such differences may be due to the facts that: (1) FDG uptake depends on both the density and the glucose metabolism of the cells; (2) when several types of cells in the lesion are activated, FDG uptake is related to the total number of them. In our model, Allaire et al previously showed that the activation markers ICAM-1 and LFA-1 correlated with the density of total inflammatory cells.[20] Accordingly in our study, FDG-SUV only correlated with summed ED1+ and CD8+ cells, but not to either ED1+ or CD8+ cells separately, suggesting that both monocytes and lymphocytes are involved in the FDG signal. It is also probable that other cell types, such as lymphocyte subtypes, activated endothelial cells, or fibroblasts, also participate in FDG uptake in lesions.

18F-FCH imaging of inflammatory lesions. Choline is taken up into cells by specific transport mechanisms, phosphorylated by choline kinase, metabolized to phosphatidylcholine, and incorporated into the intracellular and plasma membranes.[29] Increased choline uptake has been shown in tumors and soft tissue infection[30] and in atherosclerotic plaques.[14,15] It is a cell proliferation marker, since both

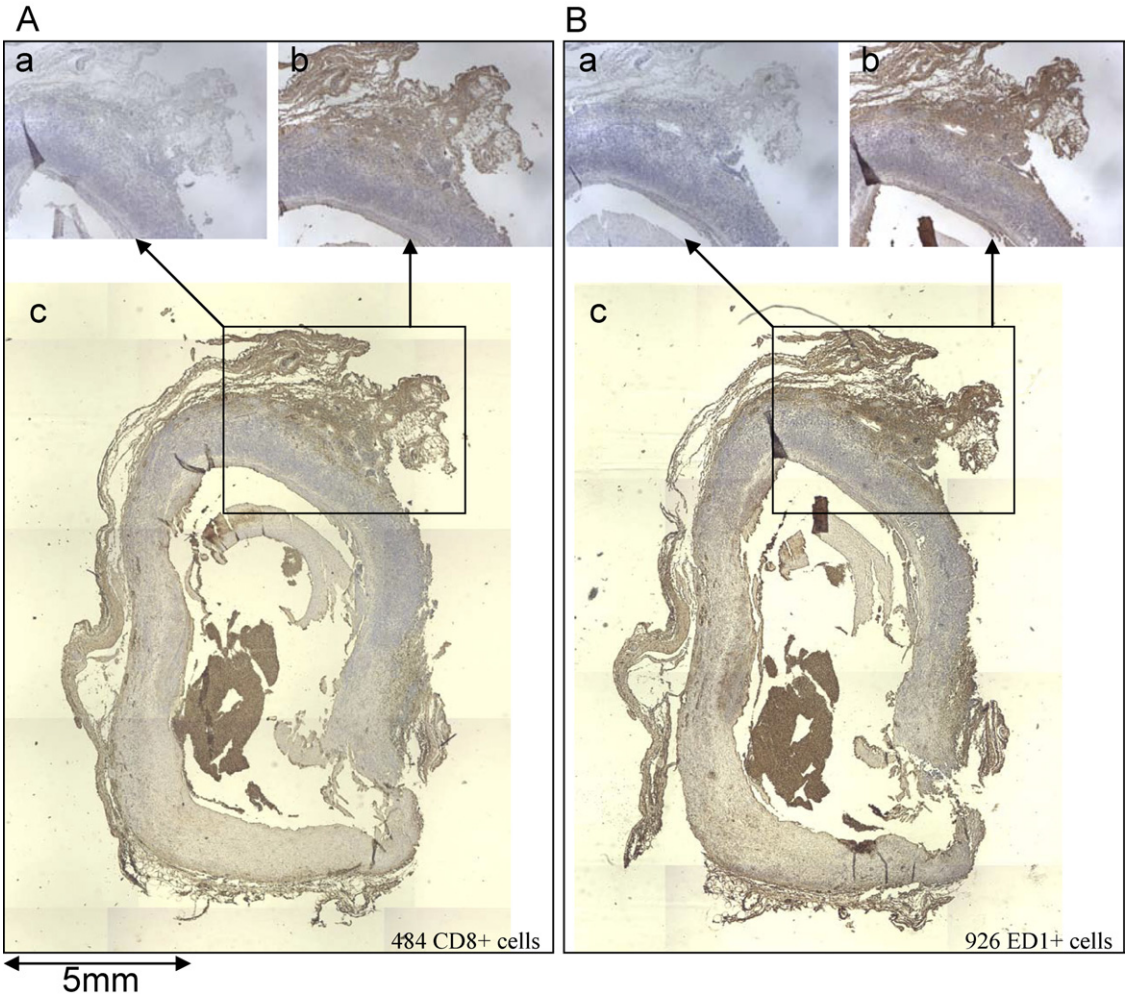

Fig 4. Immunohistology of an abdominal aortic aneurysm (AAA). Adventitial CD8 **(A)** and ED1 **(B)** stainings in a large AAA. **a,** Negative control. **b,** Corresponding stained area. **c,** Whole AAA section staining.

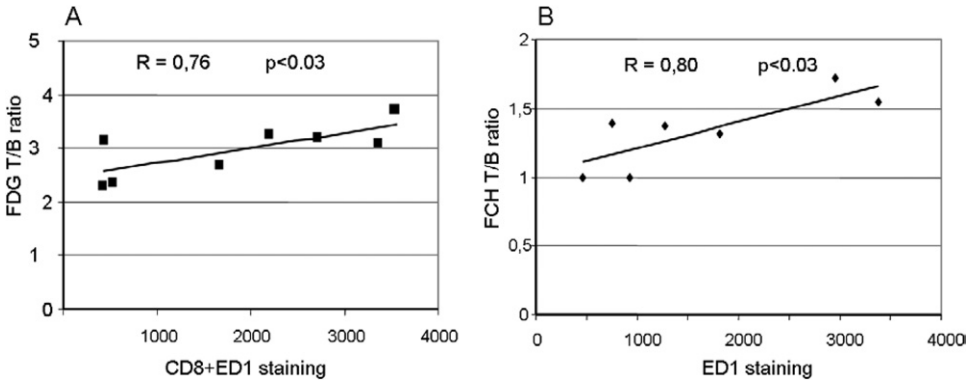

Fig 5. Relation between positron-emission tomography (PET) images quantification and number of leukocytes on histology. *T/B ratio*, Ratio of SUV_{max} in abdominal aortic aneurysm (AAA) to SUV_{max} in surrounding tissue vs CD8; *ED1*, number of stained cells per tissue sections.

choline transporters and choline kinase, which triggers the metabolic pathway leading to choline incorporation into membranes, are upregulated in highly proliferative cells.[31] However, choline influx was also evidenced in murine macrophages stimulated by colony stimulating factor-1, and in human monocytic THP-1 cells in vitro.[32] According to our data, a good correlation was previously found between FCH or 11C-choline accumulation and ED1 staining in murine atherosclerotic plaques ex vivo.[14,33,34] Moreover, Matter et al also reported that the FCH signal is better correlated to the presence of macrophages than that of FDG. But our results point out the fact that target-to-background ratios on FCH-PET are inferior to those obtained with FDG in AAAs. We found less accumulation in lesions, possibly because of a lower uptake of choline than glucose in activated cells, as previously reported in experimental aseptic inflammation.[30]

18F-DPA714 imaging of inflammatory lesions. PBRs are heterotrimers (isoquinoline binding protein; a voltage-dependent anion channel and an adenine nucleotide transporter) located primarily on mitochondrial membranes of various cells, especially glial cells in the brain, and inflammatory cells.[35] In experimental cerebral ischemia, high densities of PBR correlate with the infiltration of macrophages. DPA (N,N-diethyl-2-[2-(4-methoxyphenyl)-5,7dimethylpyrazolo[1,5-a]pyrimidine-3-yl]acetamide) was recently developed as a PBR ligand and radiolabeled with C-11 (DPA713) and F-18 (DPA714).[16,17] Our data suggest specific 18F-DPA714 uptake in both inflammatory AAA wall and in normal aortic wall. Indeed, PBRs are abundant in endothelial cells, striated muscle cells in the heart, smooth muscle cells of the blood vessels, and mast cells[35]; this probably explains our findings as also suggested by Laitinen et al in mice.[36] In another report, an increase in PBR density was reported in human atheromatous plaque using 3H-PK11195 autoradiography after endarterectomy,[37] but no comparison to normal aorta could be made in this study. Very recently, in vivo detection of giant cell arteritis and Takayasu arteritis were reported using 11C-PK11195 PET in seven patients[38,39] that had not been evidenced using FDG. The discrepancy between the results in these patients and the present study in rats may be explained by a difference in PBR expression according to the type of cells in lesions (macrophages and lymphocytes in rat aneurysms, giant multinucleated cells and activated fibroblasts in giant cell arteritis and Takayashu arteritis), or a difference in the molecular targets of 11C-PK11195 and 18F-DPA714.

Potential clinical relevance of our findings. Human AAA is a spatiotemporal model of atherothrombotic disease, including an intraluminal thrombus, aortic wall degradation, angiogenesis, and adventitial inflammatory response,[6] which all have been linked to AAA enlargement.[40] Our rat model is relevant to all of these processes, especially to the adventitial immune response observed in outer media and adventitia (predominantly mononuclear cells, including lymphocytes).[6,20] Like in atherosclerotic plaques, the question of clinical interest is whether or not biological processes (especially leukocytes infiltration and activation that lead to release of proteases) are active or not in AAA parietal wall (ie, if AAA is at risk for rapid enlargement or not).[12] Because of its higher sensitivity of detection, FDG is a very good candidate for activated leukocytes imaging in AAA despite a lower specificity than FCH. In theory, the best tracer for prognostic evaluation of AAA in patients would be the one better correlated to AAA development. To this issue, encouraging data were previously reported suggesting that FDG is linked to myocardial infarction and stroke in atherosclerotic patients,[10,11] as well as to AAA evolvement.[12,13] Other radiotracers, such as markers of thrombotic or fibrinolytic activity, may also be of interest to predict risk of atherosclerotic plaques and AAA evolvement,[19] especially 99mTc-annexin A5.[41,42] But they will have to be compared to FDG and FCH, both in terms of sensitivity of detection and prediction of events.

Limits of the study. Partial volume effects induce an underestimation of measurements in PET images (no correction was applied in this study), probably inducing underestimation of SUV_{max} values in infrarenal aorta of the grafted rats with no AAA, because of very thin aortic wall ($<<1$ mm). Attenuation correction of PET images could not be applied. Despite these limitations, signals could be seen, quantified, and well-correlated with autoradiography and histology. For FDG and FCH, the parameter that correlated best with leukocytes accumulation was the ratio of SUV_{max} in AAA wall to SUV_{max} in adjacent soft tissue. It is possibly less accurate than SUV_{max} in AAA/SUV_{mean} in arterial lumen, which is a good criteria in patients.[28] However, we could not obtain such measures since the cardiac area was out of the field of view, and the rat aortic lumen is too small for accurate measurements. For DPA714, the reason for no detection is most probably related to high specific binding in normal aorta impairing discrimination between normal and inflamed aortic wall (aneurysm-to-normal aorta activity ratio was only 2.0 ± 0.4 on autoradiography) than to methodological reasons. It is possible that imaging in patients performs better than in rats because of larger size of organs.

CONCLUSIONS

In rat experimental AAA, characterized by an important aortic wall leukocytes activity, FDG-PET showed higher sensitivity than FCH-PET to detect activated leukocytes, and 18F-DPA714-PET was negative probably because of high PBR density in both normal and pathologic vessel walls as evidenced on ex-vivo tissue binding assays.

The authors acknowledge Charbel Merheb and Aurélie Ngo for their assistance during PET experiments in Tenon Laboratory, and Mary Osborn for editing the manuscript.

AUTHOR CONTRIBUTIONS

Conception and design: LS-M, DLG
Analysis and interpretation: LS-M, RB
Data collection: LS-M, J-MA, RB, FH
Writing the article: LS-M, J-BM
Critical revision of the article: FM, BT, J-BM, DLG
Final approval of the article: LS-M, J-BM, DLG
Statistical analysis: LS-M
Obtained funding: J-BM, DLG
Overall responsibility: LS-M

REFERENCES

1. Bengtsson H, Sonesson B, Bergqvist D. Incidence and prevalence of abdominal aortic aneurysms, estimated by necropsy studies and population screening by ultrasound. Ann N Y Acad Sci 1996;800:1-24.
2. Sakalihasan N, Limet R, Defawe OD. Abdominal aortic aneurysm. Lancet 2005;365:1577-89.
3. Limet R, Sakalihassan N, Albert A. Determination of the expansion rate and incidence of rupture of abdominal aortic aneurysms. J Vasc Surg 1991;14: 540-8.
4. Kurvers H, Veith FJ, Lipsitz EC, Ohki T, Gargiulo NJ, Cayne NS, et al. Discontinuous, staccato growth of abdominal aortic aneurysms. J Am Coll Surg 2004;199:709-15.
5. Michel J-B, Martin-Ventura J-L, Egido J, Sakalihasan N, Treska V, Lindholt J, et al. Novel aspects of the pathogenesis of aneurysms of the abdominal aorta in humans. Cardiovasc Res 2011 avril 1, 1990;1:18-27.
6. Michel J-B, Thaunat O, Houard X, Meilhac O, Caligiuri G, Nicoletti A. Topological determinants and consequences of adventitial responses to arterial wall injury. Arterioscler Thromb Vasc Biol 2007;27:1259-68.
7. Sakalihasan N, Michel JB. Functional imaging of atherosclerosis to advance vascular biology. Eur J Vasc Endovasc Surg 2009;37:728-34.
8. Basu S, Chryssikos T, Moghadam-Kia S, Zhuang H, Torigian DA, Alavi A. Positron emission tomography as a diagnostic tool in infection: present role and future possibilities. Semin Nucl Med 2009;39:36-51.
9. Sheikine Y, Akram K. FDG-PET imaging of atherosclerosis: do we know what we see? Atherosclerosis 2010;211:371-80.
10. Arauz A, Hoyos L, Zenteno M, Mendoza R, Alexanderson E. Carotid plaque inflammation detected by 18F-fluorodeoxyglucose-positron emission tomography. Pilot study. Clin Neurol Neurosurg 2007;109:409-12.
11. Paulmier B, Duet M, Khayat R, Pierquet-Ghazzar N, Laissy J-P, Maunoury C, et al. Arterial wall uptake of fluorodeoxyglucose on PET imaging in stable cancer disease patients indicates higher risk for cardiovascular events. J Nucl Cardiol 2008;15:209-17.
12. Sakalihasan N, Van Damme H, Gomez P, Rigo P, Lapiere CM, Nusgens B, et al. Positron emission tomography (PET) evaluation of abdominal aortic aneurysm (AAA). Eur J Vasc Endovasc Surg 2002;23:431-6.
13. Reeps C, Essler M, Pelisek J, Seidl S, Eckstein H-H, Krause B-J. Increased 18F-fluorodeoxyglucose uptake in abdominal aortic aneurysms in positron emission/computed tomography is associated with inflammation, aortic wall instability, and acute symptoms. J Vasc Surg 2008;48:417-23; discussion: 424.
14. Matter CM, Wyss MT, Meier P, Späth N, von Lukowicz T, Lohmann C, et al. 18F-choline images murine atherosclerotic plaques ex vivo. Arterioscler Thromb Vasc Biol 2006;26:584-9.
15. Bucerius J, Schmaljohann J, Böhm I, Palmedo H, Guhlke S, Tiemann K, et al. Feasibility of 18F-fluoromethylcholine PET/CT for imaging of vessel wall alterations in humans–first results. Eur J Nucl Med Mol Imaging 2008;35:815-20.
16. Chauveau F, Boutin H, Van Camp N, Dollé F, Tavitian B. Nuclear imaging of neuroinflammation: a comprehensive review of [11C]PK11195 challengers. Eur J Nucl Med Mol Imaging 2008;35:2304-19.
17. Chauveau F, Van Camp N, Dollé F, Kuhnast B, Hinnen F, Damont A, et al. Comparative evaluation of the translocator protein radioligands 11C-DPA-713, 18F-DPA-714, and 11C-PK11195 in a rat model of acute neuroinflammation. J Nucl Med 2009;50:468-76.
18. Allaire E, Bruneval P, Mandet C, Becquemin JP, Michel JB. The immunogenicity of the extracellular matrix in arterial xenografts. Surgery 1997;122:73-81.
19. Touat Z, Ollivier V, Dai J, Huisse M-G, Bezeaud A, Sebbag U, et al. Renewal of mural thrombus releases plasma markers and is involved in aortic abdominal aneurysm evolution. Am J Pathol 2006;168:1022-30.
20. Allaire E, Mandet C, Bruneval P, Bensenane S, Becquemin JP, Michel JB. Cell and extracellular matrix rejection in arterial concordant and discordant xenografts in the rat. Transplantation 1996;62:794-803.
21. Allaire E, Guettier C, Bruneval P, Plissonnier D, Michel JB. Cell-free arterial grafts: morphologic characteristics of aortic isografts, allografts, and xenografts in rats. J Vasc Surg 1994;19:446-56.
22. Rudd JHF, Myers KS, Bansilal S, Machac J, Pinto CA, Tong C, et al. Atherosclerosis inflammation imaging with 18F-FDG PET: carotid, iliac, and femoral uptake reproducibility, quantification methods, and recommendations. J Nucl Med 2008;49:871-8.
23. Fu Y, Maianu L, Melbert BR, Garvey WT. Facilitative glucose transporter gene expression in human lymphocytes, monocytes, and macrophages: a role for GLUT isoforms 1, 3, and 5 in the immune response and foam cell formation. Blood Cells Mol Dis 2004;32:182-90.
24. Ishimori T, Saga T, Mamede M, Kobayashi H, Higashi T, Nakamoto Y, et al. Increased (18)F-FDG uptake in a model of inflammation: concanavalin A-mediated lymphocyte activation. J Nucl Med 2002;43:658-63.
25. Brewer S, McPherson M, Fujiwara D, Turovskaya O, Ziring D, Chen L, et al. Molecular imaging of murine intestinal inflammation with 2-deoxy-2-[18F]fluoro-D-glucose and positron emission tomography. Gastroenterology 2008;135:744-55.
26. Tawakol A, Migrino RQ, Bashian GG, Bedri S, Vermylen D, Cury RC, et al. In vivo 18F-fluorodeoxyglucose positron emission tomography imaging provides a noninvasive measure of carotid plaque inflammation in patients. J Am Coll Cardiol 2006;48:1818-24.
27. Hyafil F, Cornily J-C, Rudd JHF, Machac J, Feldman LJ, Fayad ZA. Quantification of inflammation within rabbit atherosclerotic plaques using the macrophage-specific CT contrast agent N1177: a comparison with 18F-FDG PET/CT and histology. J Nucl Med 2009;50:959-65.
28. Joly L, Djaballah W, Koehl G, Mandry D, Dolivet G, Marie P-Y, et al. Aortic inflammation, as assessed by hybrid FDG-PET/CT imaging, is associated with enhanced aortic stiffness in addition to concurrent calcification. Eur J Nucl Med Mol Imaging 2009;36:979-85.
29. Michel V, Yuan Z, Ramsubir S, Bakovic M. Choline transport for phospholipid synthesis. Exp Biol Med (Maywood) 2006;231:490-504.
30. Kubota K, Furumoto S, Iwata R, Fukuda H, Kawamura K, Ishiwata K. Comparison of 18F-fluoromethylcholine and 2-deoxy-D-glucose in the distribution of tumor and inflammation. Ann Nucl Med 2006;20:527-33.
31. Eliyahu G, Kreizman T, Degani H. Phosphocholine as a biomarker of breast cancer: molecular and biochemical studies. Int J Cancer 2007;120:1721-30.
32. Fullerton MD, Wagner L, Yuan Z, Bakovic M. Impaired trafficking of choline transporter-like protein-1 at plasma membrane and inhibition of choline transport in THP-1 monocyte-derived macrophages. Am J Physiol Cell Physiol 2006;290:C1230-8.
33. Kato K, Schober O, Ikeda M, Schäfers M, Ishigaki T, Kies P, et al. Evaluation and comparison of 11C-choline uptake and calcification in aortic and common carotid arterial walls with combined PET/CT. Eur J Nucl Med Mol Imaging 2009;36:1622-8.
34. Laitinen IE, Luoto P, Någren K, Marjamäki PM, Silvola JM, Hellberg S, et al. Uptake of 11C-choline in mouse atherosclerotic plaques. J Nucl Med 2010; 51:798-802.
35. Canat X, Carayon P, Bouaboula M, Cahard D, Shire D, Roque C, et al. Distribution profile and properties of peripheral-type benzodiazepine receptors on human hemopoietic cells. Life Sci 1993;52:107-18.
36. Laitinen I, Marjamäki P, Någren K, Laine VJO, Wilson I, Leppänen P, et al. Uptake of inflammatory cell marker [11C]PK11195 into mouse atherosclerotic plaques. Eur J Nucl Med Mol Imaging 2009;36:73-80.
37. Fujimura Y, Hwang PM, Trout Iii H, Kozloff L, Imaizumi M, Innis RB, et al. Increased peripheral benzodiazepine receptors in arterial plaque of patients with atherosclerosis: an autoradiographic study with [(3)H]PK 11195. Atherosclerosis 2008;201:108-11.
38. Gaemperli O, Boyle JJ, Rimoldi OE, Mason JC, Camici PG. Molecular imaging of vascular inflammation. Eur J Nucl Med Mol Imaging 2010;37:1236.
39. Pugliese F, Gaemperli O, Kinderlerer AR, Lamare F, Shalhoub J, Davies AH, et al. Imaging of vascular inflammation with [11C]-PK11195 and positron emission tomography/computed tomography angiography. J Am Coll Cardiol 2010;56:653-61.
40. Rizas KD, Ippagunta N, Tilson MD 3rd. Immune cells and molecular mediators in the pathogenesis of the abdominal aortic aneurysm. Cardiol Rev 2009;17:201-10.
41. Sarda-Mantel L, Coutard M, Rouzet F, Raguin O, Vrigneaud JM, Hervatin F, et al. 99mTc-annexin-V functional imaging of luminal thrombus activity in abdominal aortic aneurysms. Arterioscler Thromb Vasc Biol 2006;26:2153-9.
42. Kolodgie FD, Petrov A, Virmani R, Narula N, Verjans JW, Weber DK, et al. Targeting of apoptotic macrophages and experimental atheroma with radiolabeled annexin V: a technique with potential for noninvasive imaging of vulnerable plaque. Circulation 2003;108:3134-9.

Submitted Nov 3, 2011; accepted Jan 29, 2012.